

Experimental and DFT Studies Explain Solvent Control of C–H Activation and Product Selectivity in the Rh(III)-Catalyzed Formation of Neutral and Cationic Heterocycles

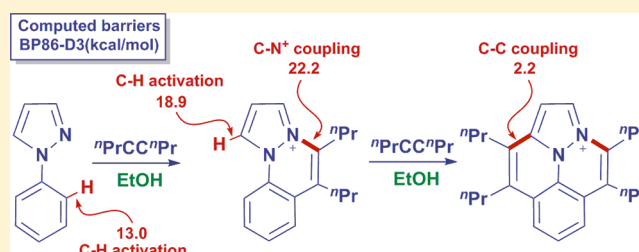
David L. Davies,^{*,†} Charles E. Ellul,[†] Stuart A. Macgregor,^{*,‡} Claire L. McMullin,[‡] and Kuldip Singh[†]

[†]Department of Chemistry, University of Leicester, Leicester, LE1 7RH, United Kingdom

[‡]Institute of Chemical Sciences, Heriot-Watt University, Edinburgh, EH14 4AS, United Kingdom

Supporting Information

ABSTRACT: A range of novel heterocyclic cations have been synthesized by the Rh(III)-catalyzed oxidative C–N and C–C coupling of 1-phenylpyrazole, 2-phenylpyridine, and 2-vinylpyridine with alkynes (4-octyne and diphenylacetylene). The reactions proceed via initial C–H activation, alkyne insertion, and reductive coupling, and all three of these steps are sensitive to the substrates involved and the reaction conditions. Density functional theory (DFT) calculations show that C–H activation can proceed via a heteroatom-directed process that involves displacement of acetate by the neutral substrate to form charged intermediates. This step (which leads to cationic C–N coupled products) is therefore favored by more polar solvents. An alternative non-directed C–H activation is also possible that does not involve acetate displacement and so becomes favored in low polarity solvents, leading to C–C coupled products. Alkyne insertion is generally more favorable for diphenylacetylene over 4-octyne, but the reverse is true of the reductive coupling step. The diphenylacetylene moiety can also stabilize unsaturated seven-membered rhodacycle intermediates through extra interaction with one of the Ph substituents. With 1-phenylpyrazole this effect is sufficient to suppress the final C–N reductive coupling. A comparison of a series of seven-membered rhodacycles indicates the barrier to coupling is highly sensitive to the two groups involved and follows the trend C–N⁺ > C–N > C–C (i.e., involving the formation of cationic C–N, neutral C–N, and neutral C–C coupled products, respectively).



1. INTRODUCTION

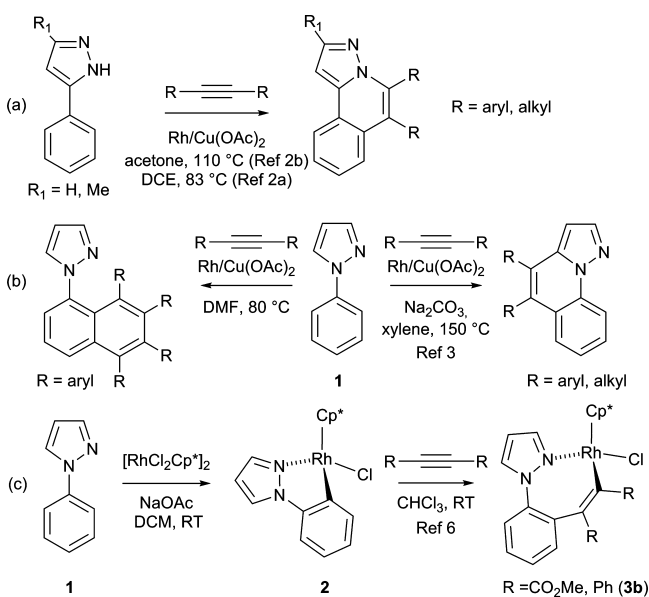
Methods to form polycyclic heterocycles through the construction of C–Y bonds (Y = C, N and O) are of vital importance for the synthesis of molecules targeting applications in pharmaceuticals and materials science. Moreover, new processes that realize this goal via the direct functionalization of C–H bonds are particularly desirable, as they avoid the prefunctionalization of the coupling partners and so benefit from an inherently improved atom economy. Among the range of late transition metals used for such catalytic C–H functionalization, dramatic progress has been made recently in Rh-catalyzed oxidative coupling, with high selectivity and functional group tolerance affording a variety of C–Y coupled products.¹ In this regard the behavior of phenylpyrazoles presents some interesting contrasts. We and others recently demonstrated that the Rh- and Ru-catalyzed reactions of 3-phenylpyrazoles with internal alkynes lead to C–N coupled heterocycles (Scheme 1a).² However, with 1-phenylpyrazole (1, Scheme 1b) only C–C coupled heterocycles have been reported to date; moreover the precise outcome depends on both the nature of the alkyne and the solvent.³ Previous studies from our groups have provided some mechanistic insight into the behavior of 1-phenylpyrazole. This species undergoes

acetate-assisted C–H activation with both $[MCl_2Cp^*]_2$ (M = Rh, Ir) and $[RuCl_2(p\text{-cymene})]_2$ to form cyclometalated products (see Scheme 1c for the Rh complex, 2). These can then readily (room temperature) undergo insertion of either dimethylacetylene dicarboxylate or diphenylacetylene into the M–C bond to give seven-membered rhodacycles.⁴ No evidence for any subsequent C–N bond coupling to form a cationic heterocycle was seen. Indeed, it has been suggested that C–N coupling might only occur with anionic directing groups that result in neutral heterocycles.^{1d} However, recently a number of groups have shown that cationic C–N coupled products can be formed with the involvement of a neutral directing group.⁵ The balance between C–C bond formation (to neutral products) and C–N bond formation (to cationic products) can be subtle, with Li and co-workers highlighting the role of the nature of the carboxylate and silver salts employed.^{5j} In earlier work Pfeffer et al. showed that alkyne insertion into cycloruthenated *N,N*-dimethylbenzylamine gave seven-membered heterocycles with electron-withdrawing substituents on the alkyne but gave C–N coupling with electron-rich alkynes.⁶ Hence, the effect of a

Received: May 10, 2015

Published: June 26, 2015

Scheme 1. Different Outcomes from the Reactions of Phenylpyrazoles with Alkynes at Rh(III)

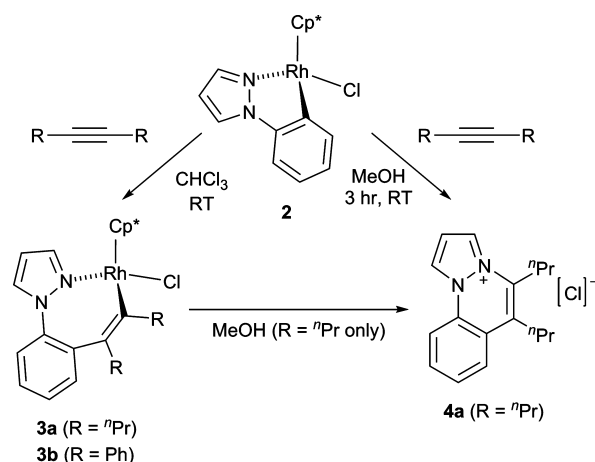


range of factors including alkyne substituents, solvent, additives, and directing group on the selectivity between C–N and C–C coupling are poorly understood.

Density functional theory (DFT) calculations on C–H activation assisted by a heteroatom directing group suggest the formation of cyclometalated **2** will involve a carboxylate-assisted (AMLA/CMD) process.^{7,8} We have also highlighted the subtleties of modeling the energetics associated with the full C–H activation and functionalization catalytic cycle.^{2a,9} Herein, we report new C–N and C–C coupling reactions of 1-phenylpyrazole, **1**, that result in the formation of cationic tricyclic and tetracyclic heterocyclic products. We also extend our study to the reactions of 2-phenylpyridine, **8**, and 2-vinylpyridine, **9**, for which only C–N coupling is observed. DFT studies provide further mechanistic insight and in combination with experiment offer a rationale for the observed product selectivities. These reaction outcomes are sensitive to the combination of the heterocyclic and alkyne substrates involved as well as the choice of solvent and counterion. Understanding the interplay of these reaction variables is vital in the design of new catalytic processes for C–H functionalization that, as well as being efficient, must also allow control in product selectivity.

2. EXPERIMENTAL STUDIES

The different outcomes seen in the reactions of alkynes with 1-phenylpyrazole (Scheme 1b) prompted us to examine the reaction of the key C–H activated intermediate **2** with 4-octyne (a, Scheme 2). Remarkably, in MeOH a further new product, the cationic heterocycle **4a**, was obtained as a result of C–N coupling, in contrast to the C–C coupling processes previously reported in DMF and xylene. **4a** was obtained in quantitative yield at room temperature within 3 h, with no observable intermediates and was fully characterized by NMR spectroscopy and by single-crystal X-ray diffraction (see Supporting Information). Repeating the same reaction in chloroform gave only slow insertion of 4-octyne to form the seven-membered rhodacycle (**3a**), as observed previously with diphenylacetylene (**3b**).⁴ However, redissolving **3a** in methanol led to reductive

Scheme 2. Stoichiometric Reactions of C–H Activated Intermediate **2** with Alkynes

elimination and formation of **4a**. This probably reflects a greater ease of chloride dissociation in MeOH, forming a vacant site and so facilitating the reductive elimination from a 16e intermediate. Despite this, the diphenylacetylene complex **3b** showed no evidence for reductive elimination even after heating in MeOH at 60 °C for 24 h.

Based on these results we investigated the catalytic formation of **4a**, initially in EtOH (see Table 1). Treatment of **1** with 1 equiv of 4-octyne and KPF₆ with [RhCl₂Cp*]₂ (5 mol % Rh) as catalyst and Cu(OAc)₂·H₂O as oxidant, provided **4a** in 78% yield in only 1 h (entry 1). Use of the cationic Rh precursor [Rh(MeCN)₃Cp*][PF₆]₂ gave a slightly higher yield (entry 2), while entry 3 shows that Rh is essential. The addition of base

Table 1. Rh-Catalyzed Heterocycle Formation with 1-Phenylpyrazole, **1**, and 4-octyne (a)^a

entry	catalyst	solvent	equiv alkyne	time (hrs)	yield (%)	
					4a	5aa
1	A	EtOH	1.2	1	78	–
2	B	EtOH	1.2	1	88	–
3	None	EtOH	1.2	16	trace	–
4 ^b	B	EtOH	1.2	1	69	7
5 ^c	B	EtOH	1.2	1	75	4
6	A	DCE	1.2	16	–	72 ^d
7	B	DCE	2.2	1	3	58
8	B	DCE	2.2	24	–	74
9	B	EtOH	2.2	3	82	8
10	B	EtOH	2.2	24	29	57

^aConditions: pyrazole (0.5 mmol); 4-octyne (see Table); catalysts A = [RhCl₂Cp*]₂ (2.5 mol %) and B = [Rh(NCMe)₃Cp*](PF₆)₂ (5 mol %, cf. pyrazole); Cu(OAc)₂·H₂O (1.25 mmol); KPF₆ (0.6 mmol); solvent (10 mL); 83 °C; yield determined by ¹H NMR vs 1,3,5-trimethoxybenzene (0.25 mmol). ^bNa₂CO₃ (1 mmol) ^cDABCO (0.5 mmol) ^dYield based on octyne

(Na_2CO_3 or DABCO) has no significant effect (entries 4 and 5).

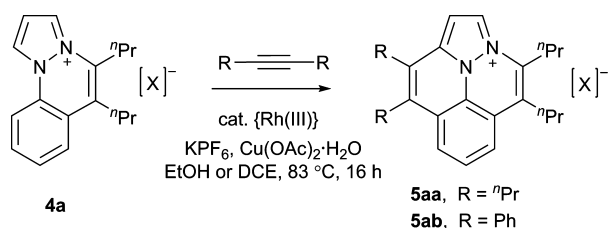
As with the stoichiometric experiments, solvent was again found to play a significant role in the product selectivity under catalytic conditions. Thus, in DCE the major species formed was not **4a**, but the new doubly inserted cationic product **5aa**, even though the alkyne is present only in slight excess (entry 6). The identity of **5aa** was confirmed by single-crystal X-ray diffraction (see [Supporting Information](#)). If the reaction was performed with 2.2 equiv of 4-octyne (entry 7), only traces of **4a** were observed even at short reaction times, the major product being **5aa**. After 24 h only **5aa** was observed (entry 8). Repeating this reaction with 2.2 equiv of 4-octyne in EtOH (entry 9) gave mainly **4a** (82%) after 3 h, but after 24 h **5aa** was the major product (57%) along with some **4a** (29%, entry 10). In contrast the corresponding reaction of 1-phenylpyrazole with PhCCPh in EtOH gave no evidence for any cationic product of type **4** and after 24 h at 120 °C only showed low conversion (14%) to a naphthylpyrazole.

Turning to the mechanism of these processes, in EtOH it seems reasonable to postulate that **4a** is an intermediate in the formation of **5aa**. In addition, the formation of **4a** is much faster than its subsequent conversion to **5aa**. In contrast, in DCE **4a** is only observed at short reaction times and then only in small amounts, suggesting that the onward conversion of **4a** to **5aa** is faster than the initial formation of **4a** itself. Conversion of **4a** to **5aa** requires a double C–H activation without any heteroatom assistance, and such processes have been reported to occur in a number of heterocycles containing acidic protons^{5,10} and recently for pyridinium and imidazolium salts.¹¹

To investigate whether direct C–H activation of **4a** is feasible, stoichiometric cyclometalation of **4a**[PF_6^-] with $[\text{RhCl}_2\text{Cp}^*]_2$ and NaOAc was attempted in MeOH. Monitoring by ^1H NMR spectroscopy showed the signals for **4a** are unchanged even after 24 h at 83 °C. Repeating the reaction in methanol- d_4 with catalytic $[\text{RhCl}_2\text{Cp}^*]_2$ led, after heating in a sealed tube at 83 °C for 48 h, to 29% deuteration at the *ortho*-H position on the phenyl ring alongside substantial deuteration at all the pyrazole ring positions. Heating **4a**[PF_6^-] in methanol- d_4 under the same conditions but with no Rh present also exchanged the pyrazole protons, but in this case no exchange was observed at the phenyl ring. Thus, the Rh catalyst can effect the non-heteroatom directed C–H activation of **4a**, but the non-observation of any cyclometalated intermediates indicates this step is thermodynamically unfavorable and so reversible.

To confirm that **4a** is an intermediate to **5aa**, isolated **4a**[PF_6^-] was used as a substrate for the catalysis with 4-octyne (see [Scheme 3](#)). Surprisingly, only very low conversions to **5aa** were observed in either EtOH (3%) or DCE (8%) after 16 h. Repeating the reactions in the presence of 1 equiv of KOAc

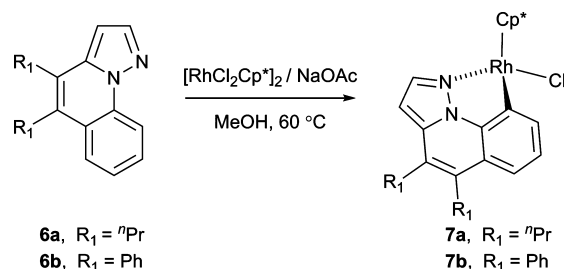
Scheme 3. Reactions of **4a with Alkynes (X = PF_6^- or OAc⁻, see text)**



increased the conversion of **4a** to **5aa** in both EtOH (54%) and DCE (99%). Similar results are observed in the reaction of **4a**[OAc⁻] with 4-octyne in either DCE or EtOH, hence the presence of a significant concentration of OAc⁻ appears to be a key requirement to form **5aa** from **4a**. Interestingly, in contrast to 1-phenylpyrazole, **4a** will also undergo C–C coupling with diphenylacetylene in the presence of KOAc to form **5ab**.

Having shown that C–N coupling to form **4a** can be followed by C–C coupling to form **5aa** and **5ab**, we considered whether the reactions could be performed in the opposite order. Thus, the alternative C–C coupled substrates, **6a** and **6b** were prepared using Miura's method^{3b} and shown to undergo acetate-assisted cyclometalation in high yield upon treatment with $[\text{RhCl}_2\text{Cp}^*]_2$ and NaOAc ([Scheme 4](#)). Both cyclometalated complexes **7a/b** were fully characterized by NMR spectroscopy and single-crystal X-ray diffraction (see [Supporting Information](#)).

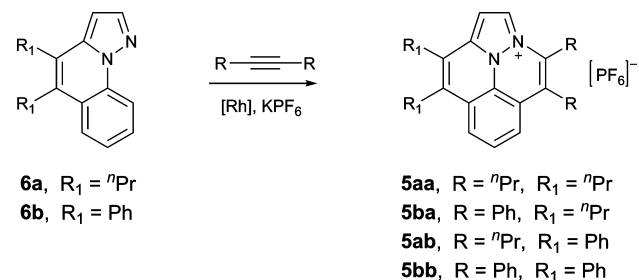
Scheme 4. Cyclometallation of **6a and **6b****



Reaction of complexes **7a/b** with 4-octyne in methanol then proceeded as for the phenylpyrazole analogue, **2** ([Scheme 2](#)), to afford cationic heterocycles **5aa** and **5ab**, respectively, in quantitative yield. However, in contrast to **2**, complexes **7a/b** also reacted, though more slowly, with diphenylacetylene in methanol to give cationic species **5ba** and **5bb**, respectively. Hence by making the substrate more rigid, the C–N coupling with diphenylacetylene will proceed. In none of these reactions was there any evidence of a seven-membered ring insertion intermediate similar to **3**.

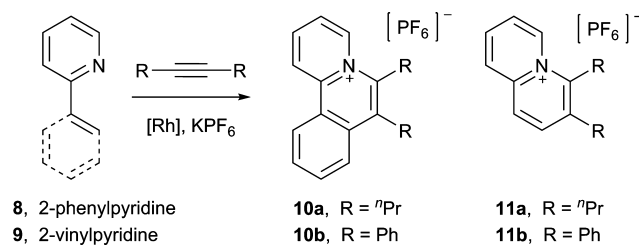
The catalytic conversion of substrates **6** to tetracyclic cations **5** was also tested, and the results are shown in [Table 2](#). As found in the stoichiometric reactions described above, **6a** and **6b** could be catalytically converted in good yields to **5aa** and **5ab**, respectively, by reaction with 4-octyne. The reactions with diphenylacetylene also proceeded to give **5ba** and **5bb**, respectively, but in slightly reduced yields. Formation of **5bb** is least favored, giving only a 39% yield and formation of some byproducts. The identity of salts **5ba** and **5bb** has been confirmed by X-ray crystallography (see [Supporting Information](#)).

Having investigated the reactions of 1-phenylpyrazole, we considered the effect of the heterocycle substrate on the outcome by investigating the analogous reactions with 2-phenylpyridine, **8**, and 2-vinylpyridine, **9** ([Table 3](#)). As with **1**, the reactions of **8** and **9** with 4-octyne work well ([Table 3](#), entries 1 and 3); moreover for these pyridine substrates, reaction with diphenylacetylene is also successful, giving C–N coupled products in reasonable to good yield (entries 2 and 4). The same products have been recently reported using Ru or Rh catalysis.^{5c,d,f} In contrast, all attempts to get the salts **10** to react further with alkynes to generate tetracyclic products (similar to the conversion of **4a** to **5aa/5ab**) were unsuccessful, even in

Table 2. Rh-Catalyzed Coupling of **6a** and **6b** with Alkynes^a

entry	substrate	alkyne	yield (%)
1	6a	4-octyne	85 (5aa)
2	6a	PhCCPh	52 (5ba)
3	6b	4-octyne	67 (5ab)
4	6b	PhCCPh	39 (5bb)

^aConditions: pyrazole (0.5 mmol), alkyne (1.2 mmol), [Rh-(NCMe)₃Cp*](PF₆)₂ (5 mol %), Cu(OAc)₂·H₂O (1.25 mmol), KPF₆ (0.6 mmol), 1,3,5-trimethoxybenzene (0.25 mmol), EtOH (10 mL), 83 °C, yields determined by ¹H NMR spectroscopy.

Table 3. Rh-Catalyzed Coupling of 2-phenylpyridine (**8**) and 2-vinylpyridine (**9**) with Alkynes^a

	substrate	alkyne	product	yield (%)
1	8	4-octyne	10a	72
2	8	PhCCPh	10b	61
3	9	4-octyne	11a	67
4	9	PhCCPh	11b	45

^aConditions: pyridine (0.5 mmol), alkyne (0.6 mmol), [RhCl₂Cp*]₂ 2.5 mol %, Cu(OAc)₂·H₂O (1.25 mmol), KPF₆ (0.6 mmol), EtOH (10 mL), 83 °C, 6 h, yield determined by ¹H NMR spectroscopy.

DCE which was shown to promote this process for **4a**. Thus, double C–H activation and C–C coupling are also highly dependent on the precise substrate employed.

3. COMPUTATIONAL STUDIES

In order to understand the factors determining the different product selectivities observed experimentally, density functional theory (DFT) calculations have been undertaken to establish the mechanisms and energetics of these various C–N and C–C oxidative coupling reactions. Experimentally, the reaction outcomes depend on the combinations of the alkyne, substrate, and solvent employed. Thus, with **1** in EtOH C–N coupling only occurs with 4-octyne (**a**) to give **4a**, while no equivalent C–N coupled product is seen with diphenylacetylene (**b**). In contrast, the phenyl- and vinylpyridines **8** and **9** react with both alkynes to form heterocycles **10a/b** and **11a/b**, respectively. Tetracycle formation also depends on the system involved: the C–N strapped substrate **4a** reacts with both alkynes to form **5aa** and **5ab**, and these can also be formed from the C–C strapped substrates **6a** and **6b**, from which the complementary **5ba** and **5bb** can also be accessed. In contrast, no further

reaction of the C–N coupled pyridine-based heterocycles **10a/b** and **11a/b** is seen with either alkyne. The choice of solvent also affects reactivity: in EtOH the reaction of **1** to form **4a** is faster than the onward reaction of **4a** to give **5aa**. However, in DCE the second C–C coupling to give tetracycle **5aa** competes with the initial C–N coupling with the result that **4a** does not build up significantly during catalysis.

In modeling these various processes with DFT calculations, all geometries have been optimized using the BP86 functional and a modest basis set (BS1). As in previous related work,^{2a,9} we report computed free energies, with corrections for solvation (PCM approach), dispersion (Grimme's D3 parameter set), and basis set effects (with a larger basis set, BS2, including diffuse functions). See the [Computational Details](#) section for full details.

Reactivity of 1 and 4a with Alkynes. The free energy profiles for the initial C–H activation of 1-phenylpyrazole and the subsequent coupling with 4-octyne and diphenylacetylene in EtOH are shown in [Figure 1](#). We consider Rh(OAc)₂Cp*, **A**, to be the catalytically active species formed under the reaction conditions, and so all free energies are quoted relative to this species combined with those of the relevant substrates. Cyclometalation of **1** proceeds via initial substitution of an acetate ligand in **A** to give N-bound precursor ¹**B** ($G_{\text{EtOH}} = +1.3$ kcal/mol, where the preceding superscript indicates the substrate involved), from which C–H activation proceeds in a formally two-step process via the agostic/H-bonded intermediate ¹**INT(B–C)** ($G_{\text{EtOH}} = +11.7$). C–H activation therefore has an overall barrier of 13.0 kcal/mol and gives the cyclometalated AcOH adduct, ¹**C**, at +6.2 kcal/mol.¹² The onward reaction with 4-octyne then involves AcOH substitution to give intermediate ¹**Da** ($G_{\text{EtOH}} = -5.1$ kcal/mol) followed by sequential alkyne insertion and C–N reductive coupling to give ¹**Fa** in which the heterocyclic product **4a** is bound to Rh in an η^4 -fashion. Both these steps are exergonic and have reasonable barriers of 15.1 and 22.2 kcal/mol, respectively.¹³

With diphenylacetylene an analogous mechanism is computed but with some important changes in energetics. Thus, intermediate ¹**Db** is less stable than ¹**Da**, and while the subsequent migratory insertion has a similar barrier (12.7 kcal/mol), this step becomes significantly more favorable ($\Delta G_{\text{EtOH}} = -8.8$ kcal/mol) than with 4-octyne. This result can be traced to an additional interaction between the formally unsaturated Rh center in ¹**Eb** and one of the Ph substituents (Rh–C⁹ = 2.31; Rh–C¹⁰ = 2.49 Å, see [Figure 2](#) which also defines the atom labeling scheme employed). This greater stabilization of ¹**Eb** disfavors the C–N reductive coupling which has an increased barrier of 27.3 kcal/mol and becomes endergonic by 4.3 kcal/mol. These less favorable energetics are consistent with the non-observation of any heterocyclic products experimentally with diphenylacetylene, while the facile migratory insertion is in accord with the formation of the seven-membered rhodacycle, **3b**, in the stoichiometric reactions⁴ (see [Scheme 2](#)). As no equivalent stabilization occurs with the ⁿPr substituents in ¹**Ea**, C–N reductive coupling from that species is both more kinetically accessible and exergonic and can proceed to give ultimately the heterocycle **4a**. The Rh(I) species formed in this reductive coupling step can then be reoxidized by Cu(OAc)₂ to regenerate catalytically active Rh(OAc)₂Cp*, **A**.

The onward reaction of **4a** with 4-octyne or diphenylacetylene to form tetracycles **5aa** or **5ab**, respectively, requires the double C–H bond activation of **4a** prior to the alkyne insertion

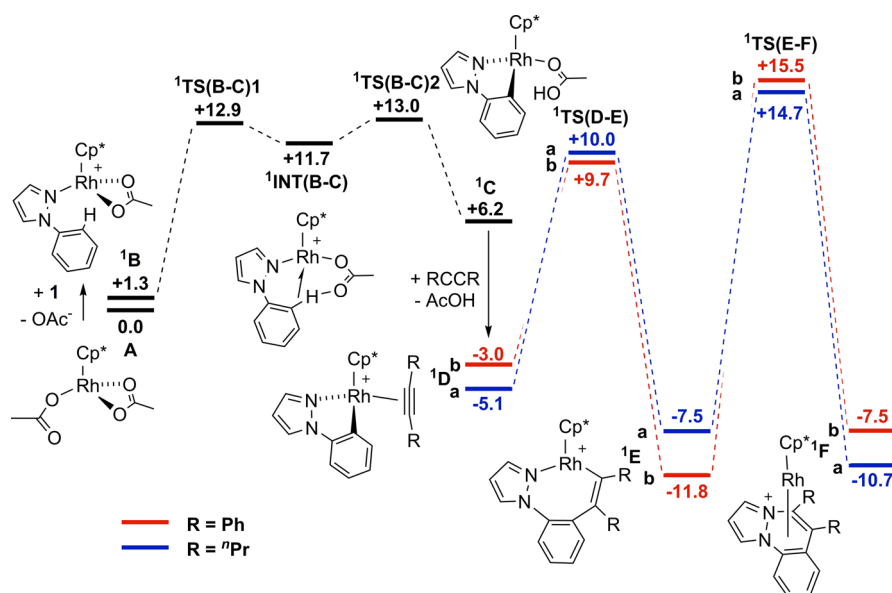


Figure 1. Computed reaction profiles (kcal/mol) for the coupling of 1-phenylpyrazole, **1**, with 4-octyne (a) and diphenylacetylene (b) at $\text{Rh}(\text{OAc})_2\text{Cp}^*$, A, in EtOH. In each case free energies are quoted relative to A and the free substrates.

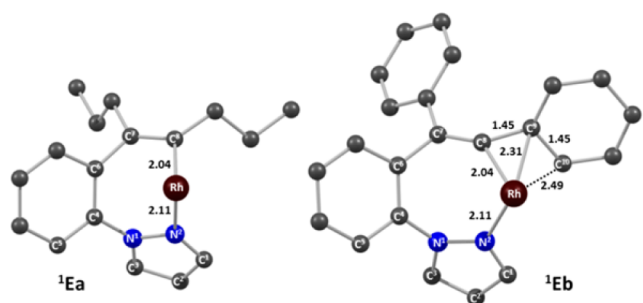


Figure 2. Computed structures of **1Ea** and **1Eb** with selected distances in Å. Structures are viewed approximately along the Rh-Cp* centroid axis, with the Cp* ligand and all H atoms omitted for clarity.

and C-C reductive coupling steps. The first C-H bond activation is necessarily a non-directed process, at either the pyrazole C³-H³ bond or the arene C⁵-H⁵ bond. The former possibility was found to be more accessible and proceeds via ^{4a}TS(A-B) at +18.9 kcal/mol (see Figures 3 and 4), 5.0 kcal/mol below that for the alternative C⁵-H⁵ bond activation (see Supporting Information). The activation of the C³-H³ bond starts from an adduct of A and 4a, A·4a, which displays a short contact of 1.91 Å between the protic H³ and O¹, the pendant oxygen of the κ^1 -OAc ligand. ^{4a}TS(A-B) then incorporates H-transfer onto oxygen (C³...H³ = 1.22 Å; O¹...H³ = 1.59 Å) with concomitant Rh-C³ bond formation (2.26 Å), a process that also requires the dissociation of one arm of the spectator acetate ligand to accommodate the new Rh-C bond (Rh...O³ = 3.44 Å cf. 2.20 Å in A·4a). After HOAc dissociation, the subsequent C⁵-H⁵ bond activation in intermediate ^{4a}B ($G_{\text{EtOH}} = -3.3$ kcal/mol) exploits the new Rh-C³ bond as a directing group and leads to the cyclometalated AcOH adduct ^{4a}C ($G_{\text{EtOH}} = +1.7$) through a regular two-step intramolecular acetate-assisted C-H activation. The reaction of A with 4a to form ^{4a}C is computed to be endergonic and to have barriers of 18.9 and 24.3 kcal/mol for the forward and reverse directions, respectively. This is consistent with the slow H/D exchange seen experimentally in the absence of alkyne, where relatively

forcing conditions are required as well as the non-observation of any cyclometalated intermediates.

From ^{4a}C the formation of **5aa** readily proceeds via substitution of AcOH by 4-octyne to give ^{4a}Da ($G_{\text{EtOH}} = -12.5$ kcal/mol) followed by insertion into the Rh-aryl bond ($\Delta G_{\text{EtOH}}^\ddagger = +16.6$ kcal/mol). This step is markedly endergonic ($\Delta G_{\text{EtOH}} = +5.8$ kcal/mol), in contrast to the equivalent step in Figure 1 (**1Da** → **1Ea**, $\Delta G_{\text{EtOH}} = -2.4$ kcal/mol), and reflects the increased rigidity imposed by the {C₂Pr₂} “strap” in the seven-membered rhodacycle ^{4a}Ea. The final C-C coupling step in ^{4a}Ea is also far more accessible than C-N bond coupling in **1Ea** and proceeds with a barrier of only 2.2 kcal/mol to give ^{4a}Fa ($G_{\text{EtOH}} = -33.0$ kcal/mol) in which the tetracyclic product **5aa** is bound in an η^4 -fashion to Rh.

The onward reaction of ^{4a}C with diphenylacetylene shows very similar energetics to those computed with 4-octyne, and in particular, the final C-C bond coupling event again has a minimal barrier (1.9 kcal/mol) and is strongly exergonic. **5ab** should therefore be readily formed, as is observed experimentally. The similar behavior of 4-octyne and diphenylacetylene with 4a is in marked contrast to their reactions with **1**. This may in part reflect the intrinsically more facile C-C coupling (involving two formally anionic C-centers) that is involved in tetracycle formation compared to the C-N coupling necessary to form **4a** (combining an anionic C with a neutral N center, see Discussion section). In addition, whereas intermediate **1Eb** was stabilized by an interaction with the alkyne phenyl substituent, no such interaction is seen in ^{4a}Eb, as the increased rigidity of the “strapped” rhodacycle does not allow the substituent to approach the Rh center (the shortest Rh...C_{phenyl} contact is to the ipso carbon, at 3.04 Å).

The marked solvent dependency of the reaction of **1** with 4-octyne prompted us to recompute the reaction profiles in Figures 1 and 3 with a correction for DCE solvent (see Supporting Information for full details). The major change is centered on the first step in the reaction of **1** that involves the displacement of an acetate anion in A by the neutral substrate to form cationic B and free acetate. This process is more accessible in EtOH ($\Delta G_{\text{EtOH}} = +1.3$ kcal/mol) than in DCE

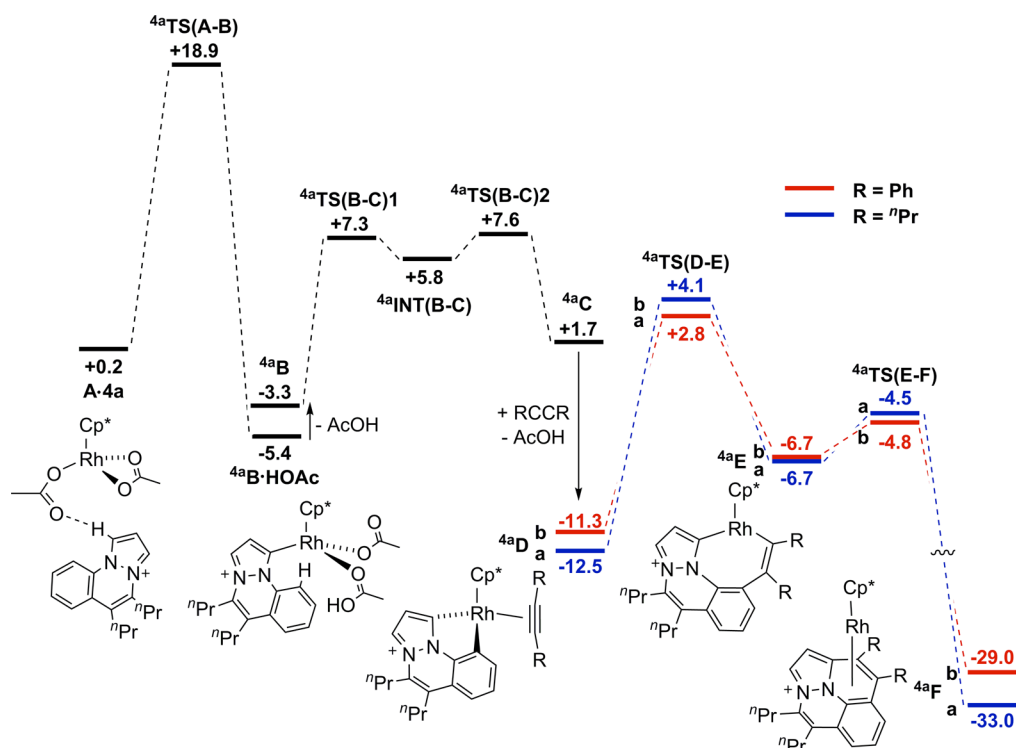


Figure 3. Computed reaction profiles (kcal/mol) for the coupling of **4a** with 4-octyne (a) and diphenylacetylene (b) at $\text{Rh}(\text{OAc})_2\text{Cp}^*$, **A**, in EtOH. In each case free energies are quoted relative to **A** and the free substrates. The structures of ^4aB , $^4\text{aINT}(\text{B-C})$, and ^4aC are analogous to ^1B , $^1\text{INT}(\text{B-C})$, and ^1C in Figure 1 and so are omitted for clarity.

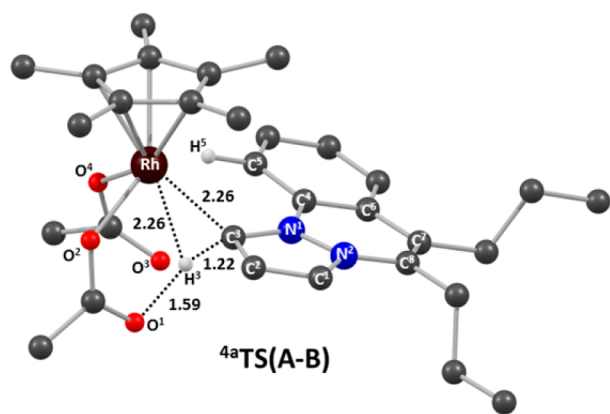


Figure 4. Computed structure of $^4\text{aTS}(\text{A-B})$ with selected distances in Å. All non-participating H atoms omitted for clarity.

($\Delta G_{\text{DCE}} = +5.9$ kcal/mol) and has the effect of raising the overall barrier to C–H activation in DCE to +17.8 kcal/mol, compared to only 13.0 kcal/mol in EtOH. In contrast, the reaction of **4a** is less solvent dependent, as in this case it is the neutral bis-OAc species **A** that effects a non-directed C–H activation without requiring any dissociation of acetate. The energy of the key transition state in this process, $^4\text{aTS}(\text{A-B})$, is therefore not significantly affected by the solvent employed ($G_{\text{EtOH}} = +18.9$ kcal/mol cf. $G_{\text{DCE}} = +19.1$ kcal/mol). Under catalytic conditions, once **4a** is formed it will be in competition with **1** for C–H activation at the catalytically active species **A**. In EtOH acetate loss and C–H activation of **1** ($\Delta G_{\text{EtOH}}^{\ddagger} = +13.0$ kcal/mol) is clearly kinetically favored over the non-directed C–H activation of **4a** at **A** ($\Delta G_{\text{EtOH}}^{\ddagger} = +18.9$ kcal/mol). Substrate **1** therefore reacts preferentially, resulting in the observed buildup of **4a** in EtOH. The onward reaction of **4a** to

give **5aa** will then only occur later in the catalysis once the concentration of **1** in solution is reduced. In DCE, however, the C–H activations of both **1** and **4a** are competitive ($\Delta G_{\text{EtOH}}^{\ddagger} = 17.8$ kcal/mol cf. $\Delta G_{\text{DCE}}^{\ddagger} = 19.1$ kcal/mol), and so as **4a** is formed, it can react on to give tetracycle **5aa**. A further factor in the more efficient onward reaction of **4a** in DCE is the greater stability of adduct **A·4a** ($G_{\text{DCE}} = -0.9$ kcal/mol) over intermediate ^1B ($G_{\text{DCE}} = +5.9$ kcal/mol) that will favor the non-directed C–H activation.¹⁴ In contrast in EtOH these two species are much closer in energy ($\Delta G_{\text{EtOH}} = 1.1$ kcal/mol). This difference reflects the greater propensity of acetate to dissociate in a more polar solvent and also explains the need for additional acetate to facilitate the formation of **5aa** from isolated **4a**.

Reactivity of 6a and 6b with Alkynes. Experimentally the neutral C–C strapped substrates **6a** and **6b** are able to react with both 4-octyne and diphenylacetylene to form (with **6a**) tetracycles **5aa** and **5ba** and (with **6b**) **5ab** and **5bb**. Thus, C–N coupling is now feasible with both alkynes, in contrast to what is observed with substrate **1**. The computed reaction profiles for the reactions of **6a** with 4-octyne and diphenylacetylene in EtOH are shown in Figure 5 (those for the reactions of **6b** are provided in the Supporting Information). The energetics of C–H activation are similar to those computed with **1**, although the more rigid structure of **6a** results in a one-step process via $^6\text{aTS}(\text{B-C})$ at +14.6 kcal/mol with no agostic intermediate being located. The energetics of HOAc/alkyne substitution and migratory insertion are again similar to those computed with **1**, although with **6a** migratory insertion is significantly endergonic for both alkynes (by ca. 5.5 kcal/mol), and the subsequent C–N coupling steps have barriers of ca. 11 kcal/mol, significantly lower than from $^1\text{Ea}/\text{b}$. This pattern of a thermodynamically uphill insertion followed

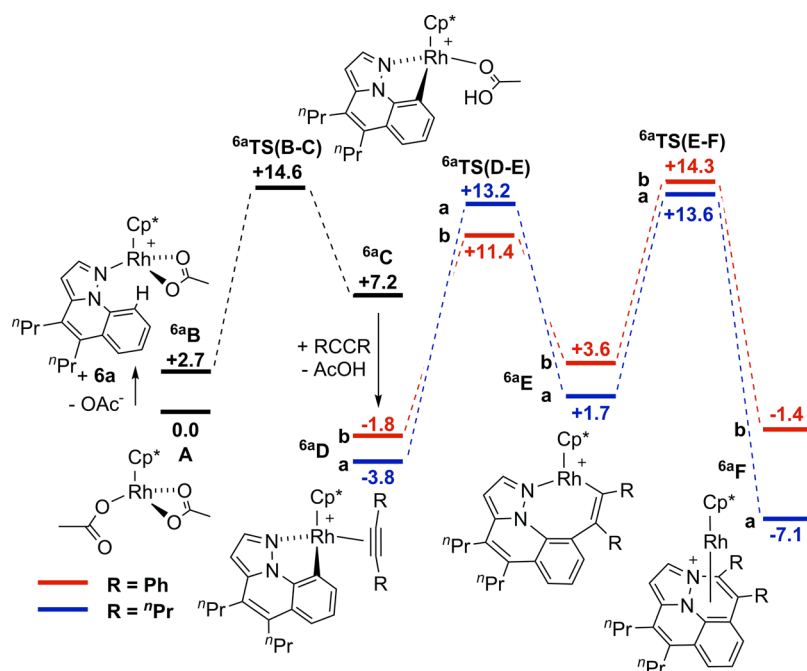


Figure 5. Computed reaction profiles (kcal/mol) for the coupling of **6a** with 4-octyne and diphenylacetylene at $\text{Rh}(\text{OAc})_2\text{Cp}^*$, **A**. Results are computed in EtOH, and free energies are quoted relative to **A** and the free substrates.

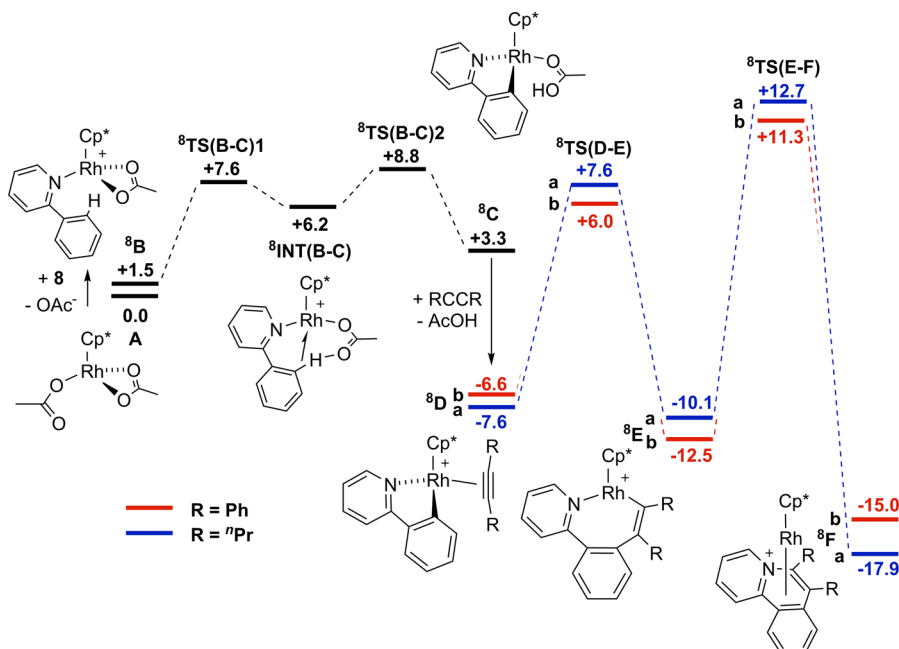


Figure 6. Computed reaction profiles (kcal/mol) for the coupling of 2-phenylpyridine, **8**, with 4-octyne and diphenylacetylene at $\text{Rh}(\text{OAc})_2\text{Cp}^*$, **A**, in EtOH. In each case free energies are quoted relative to **A** and the free substrates.

by facile reductive coupling is similar to the behavior of the C–N strapped substrate **4a**, suggesting that the rigid strap plays an important role in promoting the reaction in both cases.

The overall barriers for C–N coupling from intermediates **6aDa** and **6aDb** are 17.4 and 16.1 kcal/mol respectively, consistent with both processes readily occurring experimentally. For **6aDa** the formation of the initial product **6aFa** featuring the Rh-bound tetracycle **5aa** is exergonic by 3.3 kcal/mol, while the equivalent process with diphenylacetylene (**6aDb** → **6aFb**) is marginally uphill, and this difference may be related to the lower yield seen experimentally for **5ba** (52%) compared to **5aa**

(85%, see Table 2). The barriers for the C–N coupling step from **6aEa**/**6aEb** are ca. 10 kcal/mol higher than the equivalent C–C coupling in **4aEa**/**4aEb**, reiterating the intrinsically greater accessibility of C–C coupling when other factors are equal. We also computed the C–H activation and coupling of substrate **6b** with 4-octyne and diphenylacetylene, to give **5ba** and **5bb**. Very similar patterns to those seen in Figure 5 were found, and full details are given in the Supporting Information.

Reactions of 8 with Alkynes. In contrast to the behavior seen in the reactions of **1**, **4a**, and **6a/6b** with alkynes, 2-phenylpyridine, **8**, shows a further distinct reactivity pattern in

that it undergoes C–N coupling with both 4-octyne and diphenylacetylene, but then neither of the resultant cationic heterocycles, **10a** or **10b**, reacts further to form tetracyclic products. Similar results are seen experimentally with vinylpyridine, **9**. We focus here on the computed profiles for the reactions of 2-phenylpyridine with 4-octyne and diphenylacetylene (see Figure 6, where the data are corrected for EtOH solvent). In this case substitution of OAc[−] in **A** by substrate **8** followed by C–H activation proceeds a small overall barrier of only 8.8 kcal/mol to give, after HOAc/alkyne substitution, complexes **⁸Da** and **⁸Db** at -7.6 and -6.6 kcal/mol, respectively. As with the 1-phenylpyrazole-based substrates, the insertion barrier is slightly lower with diphenylacetylene (12.6 kcal/mol) than with 4-octyne (15.2 kcal/mol), and this step is exergonic, as was seen with the other unstrapped substrate **1**. Importantly, the C–N reductive coupling step is also exergonic (**⁸Ea** \rightarrow **⁸Fa**, $\Delta G_{\text{EtOH}} = -7.8$ kcal/mol; **⁸Eb** \rightarrow **⁸Fb**, $\Delta G_{\text{EtOH}} = -2.5$ kcal/mol), and similar barriers are now computed with both alkynes (22.8 kcal/mol from **⁸Ea** and 23.8 kcal/mol from **⁸Eb**). The computed energetics for C–N bond coupling en route to the formation of **10a** are therefore very similar to those computed for the reaction of **1** and 4-octyne (**¹Ea** \rightarrow **¹Fa**: $\Delta G_{\text{EtOH}} = -3.2$ kcal/mol; $\Delta G_{\text{EtOH}}^{\ddagger} = 22.2$ kcal/mol), while the C–N coupling to form **10b** appears to be more accessible than for **4b** (**¹Eb** \rightarrow **¹Fb**: $\Delta G_{\text{EtOH}} = +4.3$ kcal/mol; $\Delta G_{\text{EtOH}}^{\ddagger} = 27.3$ kcal/mol). The computed trends are therefore consistent with the observation of both **10a** and **10b** experimentally.

As with substrate **4a**, the potential onward reaction of **10a** or **10b** to form tetracycles requires an initial non-directed C–H activation at **A**. This step was investigated for **10a** in EtOH, and the most accessible process was found to have a barrier of 28.8 kcal/mol,¹⁵ much higher than the barrier of 18.9 kcal/mol computed for the equivalent reaction with **4a**. C–H activation is therefore significantly harder for **10a**, so much so that onward reaction to form tetracyclic products is not observed.

4. DISCUSSION

The current experimental and computational mechanistic studies detail the various outcomes of Rh-catalyzed oxidative coupling when combining different directing group substrates (1-phenylpyrazole, 2-phenylpyridine, and 2-vinylpyridine) with alkynes (4-octyne and diphenylacetylene) under varying reaction conditions (solvent and anion concentration). DFT calculations have accounted for the specific observations but also highlight some more general trends of wider relevance beyond this specific study.

Two different C–H activation processes have been characterized at Rh(OAc)₂Cp*: a standard ligand directed intramolecular C–H activation and an alternative non-directed intermolecular C–H activation. For the directed C–H activation the initial substitution of one acetate ligand by the directing group is required, resulting in the formation of charged intermediates that will be favored by more polar solvents. In contrast, the non-directed process necessitates both acetates to be bound to Rh, and the reaction therefore proceeds through neutral intermediates, the accessibility of which will be less solvent dependent. These distinctions are confirmed in Figure 7 that displays the overall barriers computed in different solvents for both the directed and non-directed C–H activation of some of the heterocyclic substrates in this study.¹⁶ For 1-phenylpyrazole, **1**, directed C–H activation is favored in both EtOH and DCE, and alkyne insertion in these systems forms

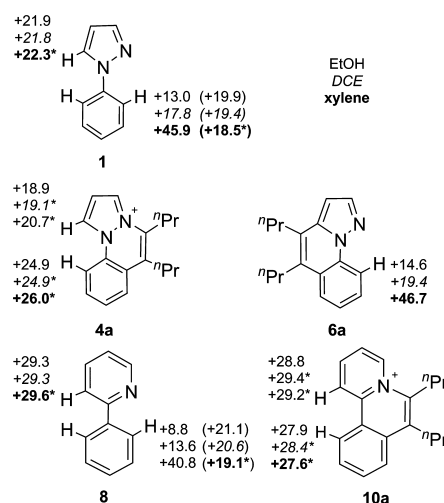


Figure 7. Computed barriers for directed and non-directed C–H activation of various heterocyclic substrates at Rh(OAc)₂Cp*. Barriers are quoted relative to the most stable precursor set 0.0 kcal/mol; this is generally Rh(OAc)₂Cp* and the free substrate except in those cases marked with an asterisk where it is a H-bonded adduct (similar to **A-4a** in the main text). Barriers are computed for EtOH (plain text), DCE (italics), and xylene (bold) solvents; values in parentheses for substrates **1** and **8** are for non-directed C–H activation at the *ortho*-C–H position of the phenyl group.¹²

seven-membered rhodacycles that are set up for C–N bond coupling to form cationic heterocyclic products. Interestingly, the alternative non-directed C–H activation also has reasonable barriers of around 22 kcal/mol at the C⁵–H⁵ bond but is actually kinetically more accessible at the backbone *ortho*-C–H bond of the phenyl group (ca. 19 kcal/mol). These values are also largely independent of the solvent, as anticipated. In the very low polarity xylene solvent, non-directed C–H activation is favored. A detailed computational study of the subsequent reaction with alkynes to give the neutral C–C coupled products reported by Miura and co-workers^{3b} (viz. substrates **6a** and **6b** used in this study) and the observed competition for the formation of naphthalene products is currently underway.

C–H activation barriers for the “strapped” substrates **4a** and **6a** are also given in Figure 7. For cationic **4a**, barriers for non-directed C–H activation of ca. 19 kcal/mol are computed in both EtOH and DCE, approximately 3 kcal/mol lower than the equivalent processes for **1**. Oxidative coupling to **5aa** and **5ab** proved possible in both solvents, although this is sensitive to the concentration of acetate (and hence the form in which this anion is introduced into the reaction) due to the need for Rh(OAc)₂Cp* to be present to effect the non-directed C–H activation. This was evident in the more efficient onward reaction of **4a** as its OAc[−] rather than its PF₆[−] salt. We would also predict that oxidative coupling should be possible in xylene. In contrast the directed C–H activation of **6a** is very solvent dependent: this is accessible in both EtOH and DCE leading ultimately to the formation of **5aa** and **5ba**. In xylene, however, directed C–H activation is not possible, and so no further reaction to tetracyclic products is seen, as was reported by Miura. 2-phenylpyridine, **8**, has the lowest barrier to directed C–H activation of those substrates considered here, but then in contrast, isoquinolinium **10a** has the highest barriers to non-directed C–H activation, even when the slightly lower barriers at the *ortho*-C–H position are taken into account. This seems likely to relate to the lower acidity of the backbone C–H bonds

associated with the pyridinium ring (with one electronegative nitrogen) compared to pyrazole-based **4a** with two nitrogens. NBO atomic charge calculations support this with a much reduced negative charge at the C⁵ position in **4a** ($q_C = -0.02$) compared to that in **10a** ($q_C = -0.22$), although a similar charge of +0.28 is computed at H⁵ in each case.

Comparing the two alkynes shows some subtle changes in the reaction energetics. With **1** and **8** (Figures 1 and 6) migratory insertion is always exergonic and exhibits lower barriers and is more favorable thermodynamically for diphenylacetylene compared to 4-octyne. The opposite trend then pertains for the reductive coupling, with this difference being most apparent in the reaction with **1**, where the phenyl substituent stabilizes the Rh center in the seven-membered rhodacycle, ¹**Eb**, to such an extent that reductive coupling does not occur at all. The slightly different geometry imposed on the system by the 2-phenylpyridine moiety in ⁸**Eb** reduces this extra stabilization, and exergonic reductive coupling can still occur with an accessible barrier. With substrates **4a** and **6a** (Figures 3 and 5) the extra rigidity imposed by the backbone {C₂Pr₂} “strap” destabilizes the seven-membered rhodacycles. As a result the alkyne insertion becomes endergonic, but by the same token, the final reductive coupling is facilitated; this process is again more favorable for 4-octyne compared to diphenylacetylene.

The relative reactivities of the two alkynes with **1** and **8** can also be assessed by the isodesmic reactions shown in Figure 8.

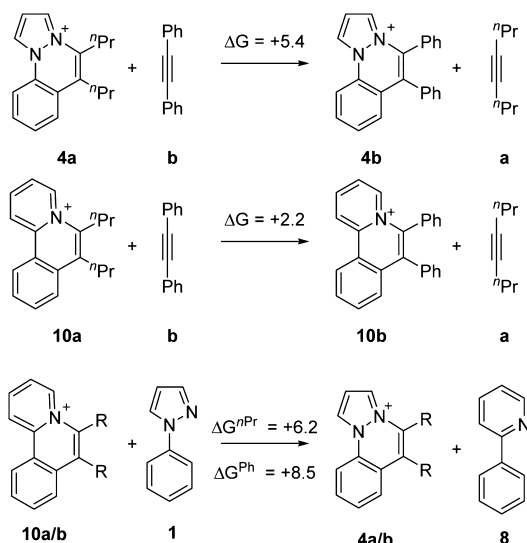


Figure 8. Calculated free energy changes (kcal/mol, in EtOH) for exchange of the alkyne moieties in **4a/4b** and **10a/10b** and the 1-phenylpyrazole and 2-phenylpyridine moieties in **10a/4a** and **10b/4b**.

The exchange of the alkyne moieties in the **4a/4b** and **10a/10b** pairs is shown to be thermodynamically uphill, indicating an intrinsic preference for the coupling reactions of 4-octyne over diphenylacetylene with both 1-phenylpyrazole and 2-phenylpyridine. It is noteworthy that this preference is slightly higher with 1-phenylpyrazole and that, experimentally, this system proved more sensitive to the alkyne identity compared to 2-phenylpyridine. Likewise exchange of the 1-phenylpyrazole and 2-phenylpyridine moieties in the **4a/10a** and **4b/10b** pairs indicates oxidative coupling is more favored with 2-phenylpyridine, probably due to the reduced ring strain in tricyclic products featuring three six-membered rings. The combination of 1-phenylpyrazole and diphenylacetylene is most disfavored, and this again fits with the difficulty in forming **4b** experimentally. These additional thermodynamic factors combine with the extra stabilization of intermediate ¹**Eb** to make the formation of **4b** inaccessible in the present system.

This and previous work allows us to monitor the ease of the final reductive coupling step as the nature of the participating groups changes. Data for five rhodacycles constructed via insertion of 4-octyne with different phenylpyrazoles are compared in Figure 9. The highest barrier ($\Delta G^\ddagger = 22.2$ kcal/mol) is for the 1-phenylpyrazole system, where a formally anionic alkenyl C couples with a neutral N to form a cationic heterocycle (“C–N⁺ coupling”). Incorporating the {C₂Pr₂} strap reduces this barrier to 11.9 kcal/mol, for the reasons discussed above. Combining anionic C and N centers to form a neutral heterocycle (C–N coupling), as in our previous study based on 5-methyl-3-phenylpyrazole (**12**), is a much easier process, with a barrier of only 9.9 kcal/mol,^{2a} less than half of that for the C–N⁺ coupling. We have also extended the current study to the coupling of two anionic C centers in ¹**Ea**, a species derived from **1** via non-directed C–H activation and alkyne insertion and a putative intermediate for the formation of species **6a**. Such C–C coupling is even more facile and is further facilitated (as was the case for C–N⁺ coupling) through the introduction of the {C₂Pr₂} strap as in ^{4a}**Ea**.

In conclusion, we have shown through experimental and computational means how a number of steps in the Rh-catalyzed oxidative coupling of N-heterocycles with alkynes can be affected by the precise substrates involved and the reaction conditions. Directed C–H activation requires substitution of acetate by the N-heterocycle and so is favored by more polar solvents. Further reaction leads to cationic tricyclic or tetracyclic products, although the ability of diphenylacetylene to stabilize a key rhodacyclic intermediate can suppress the former. Non-directed C–H activation is an energetically feasible process that, as it does not involve acetate dissociation, does not display significant solvent dependence. Hence in low polarity solvents this process becomes favored and may lead to

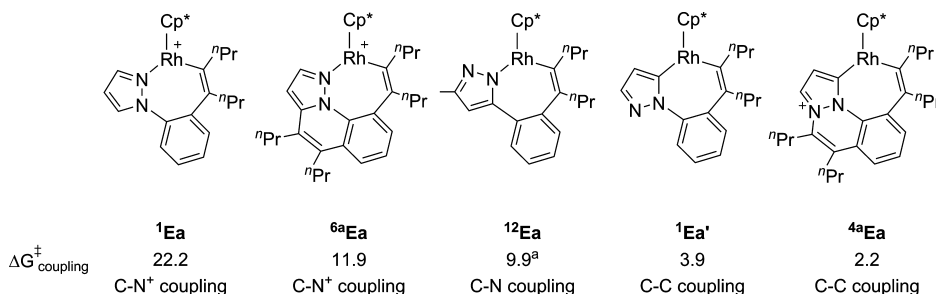


Figure 9. Computed barriers for different C–N and C–C bond coupling processes. (a) Data from ref 2a; see text for full details.

neutral C–C coupled products. Barriers for a range of key C–Y coupling events have been assessed and shown to follow the trend C–N⁺ > C–N > C–C.

5. EXPERIMENTAL SECTION

General Procedure for Catalytic C–N Coupling Reactions.

Ethanol (10 mL), substrate (0.5 mmol), and alkyne (0.6 mmol) were placed into a Schlenk tube with a stirrer bar, followed by the addition of the rhodium catalyst (0.0125 mmol, 5 mol % {Rh}), KPF₆ (0.6 mmol), and Cu(OAc)₂·H₂O (1.25 mmol). The suspension was stirred at 83 °C in an oil bath. After cooling to room temperature the product was extracted into dichloromethane (2 × 10 mL) and washed with water (20 mL) containing ethylene diamine (1 mL). The organic fraction was collected and dried over MgSO₄. The filtrate was concentrated, and the product was isolated by column chromatography using alumina eluted with ethyl acetate/methanol (100:0 to 50:50 ethyl acetate:methanol)

Computational Details. DFT calculations were run with Gaussian 03 (Revision D.01)¹⁷ and Gaussian 09 (Revision A.02).¹⁸ Rh centers were described with the Stuttgart RECPs and associated basis sets,¹⁹ and 6-31G** basis sets were used for all other atoms.²⁰ Initial BP86²¹ optimizations were performed with Gaussian 03 using the 'grid = ultrafine' option, with all stationary points being fully characterized via analytical frequency calculations as either minima (all positive eigenvalues) or transition states (one negative eigenvalue). IRC calculations and subsequent geometry optimizations were used to confirm the minima linked by each transition state. All energies were recomputed with a larger basis set, BS2, featuring cc-pVTZ on Rh and 6-311++G** on all other atoms. Corrections for the effects of ethanol ($\epsilon = 24.852$), dichloroethane ($\epsilon = 10.125$), and xylene ($\epsilon = 2.3879$) solvents were run with Gaussian 09 and used the polarizable continuum model.²² Single-point dispersion corrections to the BP86 results employed Grimme's D3 parameter set as implemented in Gaussian 09.²³

■ ASSOCIATED CONTENT

Supporting Information

Crystallographic data (CIF), full experimental details, NMR spectra, and details of all computed structures and associated energies. CCDC 1062469–1062474 contain complete crystallographic data for this paper. These data can be obtained free of charge from The Cambridge Crystallographic Data Centre via <http://www.ccdc.cam.ac.uk/pages/Home.aspx>. The Supporting Information is available free of charge on the ACS Publications website at DOI: 10.1021/jacs.5b04858.

■ AUTHOR INFORMATION

Corresponding Authors

*dld3@le.ac.uk

*s.a.macgregor@hw.ac.uk

Notes

The authors declare no competing financial interest.

■ ACKNOWLEDGMENTS

This work was supported through EPSRC awards EP/J021709/1, EP/J002917/1 (D.L.D., C.E.E.), and EP/J021911/1 (S.A.M., C.L.M.). We also thank Johnson Matthey for a loan of rhodium trichloride.

■ REFERENCES

(1) (a) Satoh, T.; Miura, M. *Chem. - Eur. J.* **2010**, *16*, 11212–11222. (b) Colby, D. A.; Tsai, A. S.; Bergman, R. G.; Ellman, J. A. *Acc. Chem. Res.* **2012**, *45*, 814–825. (c) Colby, D. A.; Bergman, R. G.; Ellman, J. A. *Chem. Rev.* **2010**, *110*, 624–655. (d) Song, G.; Wang, F.; Li, X. *Chem. Soc. Rev.* **2012**, *41*, 3651–3678. (e) Song, G.; Li, X. *Acc. Chem.*

Res. **2015**, *48*, 1007–1020. (f) Patureau, F. W.; Wencel-Delord, J.; Glorius, F. *Aldrichimica Acta* **2012**, *45*, 31–41.

(2) (a) Algarra, A. G.; Cross, W. B.; Davies, D. L.; Khamker, Q.; Macgregor, S. A.; McMullin, C. L.; Singh, K. J. *Org. Chem.* **2014**, *79*, 1954–1970. (b) Li, X.; Zhao, M. J. *Org. Chem.* **2011**, *76*, 8530–8536. (c) Ma, W.; Graczyk, K.; Ackermann, L. *Org. Lett.* **2012**, *14*, 6318–6321.

(3) (a) Umeda, N.; Tsurugi, H.; Satoh, T.; Miura, M. *Angew. Chem., Int. Ed.* **2008**, *47*, 4019–4022. (b) Umeda, N.; Hirano, K.; Satoh, T.; Shibata, N.; Sato, H.; Miura, M. *J. Org. Chem.* **2011**, *76*, 13–24.

(4) Boutadla, Y.; Davies, D. L.; Al-Duaij, O.; Fawcett, J.; Jones, R. C.; Singh, K. *Dalton Trans.* **2010**, *39*, 10447–10457.

(5) (a) Li, L.; Brennessel, W. W.; Jones, W. D. *J. Am. Chem. Soc.* **2008**, *130*, 12414–12419. (b) Zhang, G.; Yang, L.; Wang, Y.; Xie, Y.; Huang, H. *J. Am. Chem. Soc.* **2013**, *135*, 8850–8853. (c) Luo, C.-Z.; Gandeepan, P.; Jayakumar, J.; Parthasarathy, K.; Chang, Y.-W.; Cheng, C.-H. *Chem. - Eur. J.* **2013**, *19*, 14181–14186. (d) Luo, C.-Z.; Gandeepan, P.; Cheng, C.-H. *Chem. Commun.* **2013**, *49*, 8528–8530.

(e) Senthilkumar, N.; Gandeepan, P.; Jayakumar, J.; Cheng, C.-H. *Chem. Commun.* **2014**, *50*, 3106–3108. (f) Luo, C.-Z.; Jayakumar, J.; Gandeepan, P.; Wu, Y.-C.; Cheng, C.-H. *Org. Lett.* **2015**, *17*, 924–927.

(g) Muralirajan, K.; Cheng, C.-H. *Chem. - Eur. J.* **2013**, *19*, 6198–6202. (h) Jayakumar, J.; Parthasarathy, K.; Cheng, C.-H. *Angew. Chem., Int. Ed.* **2012**, *51*, 197–200. (i) Zhao, D.; Wu, Q.; Huang, X.; Song, F.; Lv, T.; You, J. *Chem. - Eur. J.* **2013**, *19*, 6239–6244. (j) Qi, Z.; Yu, S.; Li, X. *J. Org. Chem.* **2015**, *80*, 3471–3479.

(6) (a) Pfeffer, M.; Sutter, J. P.; Urriolabeitia, E. P. *Bull. Soc. Chim. Fr.* **1997**, *134*, 947–954. (b) Abbenhuis, H. C. L.; Pfeffer, M.; Sutter, J.-P.; de Cian, A.; Fischer, J.; Ji, H. L.; Nelson, J. H. *Organometallics* **1993**, *12*, 4464–4472.

(7) (a) Boutadla, Y.; Davies, D. L.; Macgregor, S. A.; Poblador-Bahamonde, A. I. *Dalton Trans.* **2009**, 5887–5893. (b) Davies, D. L.; Donald, S. M. A.; Al-Duaij, O.; Fawcett, J.; Little, C.; Macgregor, S. A. *Organometallics* **2006**, *25*, 5976–5978. (c) Davies, D. L.; Donald, S. M. A.; Al-Duaij, O.; Macgregor, S. A.; Pölleth, M. *J. Am. Chem. Soc.* **2006**, *128*, 4210–4211. (d) Davies, D. L.; Donald, S. M. A.; Macgregor, S. A. *J. Am. Chem. Soc.* **2005**, *127*, 13754–13755. (e) Guimond, N.; Gorelsky, S. I.; Fagnou, K. *J. Am. Chem. Soc.* **2011**, *133*, 6449–6457. (f) Lapointe, D.; Fagnou, K. *Chem. Lett.* **2010**, *39*, 1118–1126.

(8) For recent examples at Rh(III) see: (a) Wu, S.; Zeng, R.; Fu, C.; Yu, Y.; Zhang, X.; Ma, S. *Chem. Sci.* **2015**, *6*, 2275–2285. (b) Wu, J.-Q.; Qiu, Z.-P.; Zhang, S.-S.; Liu, J.-G.; Lao, Y.-X.; Gu, L.-Q.; Huang, Z.-S.; Li, J.; Wang, H. *Chem. Commun.* **2015**, *51*, 77–80. (c) Chen, W.-J.; Lin, Z. *Organometallics* **2015**, *34*, 309–318. (d) Li, J.; Hu, W.; Peng, Y.; Zhang, Y.; Li, J.; Zheng, W. *Organometallics* **2014**, *33*, 2150–2159.

(9) (a) Algarra, A. G.; Davies, D. L.; Khamker, Q.; Macgregor, S. A.; McMullin, C. L.; Singh, K.; Villa-Marcos, B. *Chem. - Eur. J.* **2015**, *21*, 3087–3096. (b) Carr, K. J. T.; Davies, D. L.; Macgregor, S. A.; Singh, K.; Villa-Marcos, B. *Chem. Sci.* **2014**, *5*, 2340–2346.

(10) (a) Dong, L.; Huang, J.-R.; Qu, C.-H.; Zhang, Q.-R.; Zhang, W.; Han, B.; Peng, C. *Org. Biomol. Chem.* **2013**, *11*, 6142–6149. (b) Huang, J.-R.; Zhang, Q.-R.; Qu, C.-H.; Sun, X.-H.; Dong, L.; Chen, Y.-C. *Org. Lett.* **2013**, *15*, 1878–1881. (c) Lewis, J. C.; Bergman, R. G.; Ellman, J. A. *Acc. Chem. Res.* **2008**, *41*, 1013–1025.

(11) (a) Cross, W. B.; Razak, S.; Singh, K.; Warner, A. J. *Chem. - Eur. J.* **2014**, *20*, 13203–13209. (b) Ghorai, D.; Choudhury, J. *ACS Catal.* **2015**, *5*, 2692–2696. (c) Ghorai, D.; Choudhury, J. *Chem. Commun.* **2014**, *50*, 15159–15162.

(12) An alternative transition state for deprotonation by an external acetate was also characterised and found to be less accessible ($G_{\text{EtOH}} = +23.3$ kcal/mol). Competing external deprotonation was considered for all directed C–H activation processes and was always found to be less accessible.

(13) The alternative alkyne insertions into the Rh–N bonds of ¹Da/**b** are considerably harder, with transition states approximately 19 kcal/mol above ¹TS(D-E)a/b.

(14) In the absence of a second OAc C–H activation of **4a** at cationic [Rh(OAc)Cp*]⁺ proceeds via a transition state at +34.3 kcal/

mol. An external base mechanism was more competitive in this case and involves a transition state at +20.8 kcal/mol.

(15) Non-directed C–H activation at the *ortho*-C–H bond of the phenyl group is in fact slightly more favorable in this case, although the barrier in EtOH remains high at 27.8 kcal/mol. See [Discussion](#) section.

(16) For related computational studies of non-directed C–H bond activation at Pd see: (a) Gorelsky, S. I.; Lapointe, D.; Fagnou, K. *J. Org. Chem.* **2012**, *77*, 658–668. (b) Petit, A.; Flygare, J.; Miller, A. T.; Winkel, G.; Ess, D. H. *Org. Lett.* **2012**, *14*, 3680–3683.

(17) Frisch, M. J.; Trucks, G. W.; Schlegel, H. B.; Scuseria, G. E.; Robb, M. A.; Cheeseman, J. R.; Montgomery, J. A., Jr.; Vreven, T.; Kudin, K. N.; Burant, J. C.; Millam, J. M.; Iyengar, S. S.; Tomasi, J.; Barone, V.; Mennucci, B.; Cossi, M.; Scalmani, G.; Rega, N.; Petersson, G. A.; Nakatsuji, H.; Hada, M.; Ehara, M.; Toyota, K.; Fukuda, R.; Hasegawa, J.; Ishida, M.; Nakajima, T.; Honda, Y.; Kitao, O.; Nakai, H.; Klene, M.; Li, X.; Knox, J. E.; Hratchian, H. P.; Cross, J. B.; Bakken, V.; Adamo, C.; Jaramillo, J.; Gomperts, R.; Stratmann, R. E.; Yazyev, O.; Austin, A. J.; Cammi, R.; Pomelli, C.; Ochterski, J. W.; Ayala, P. Y.; Morokuma, K.; Voth, G. A.; Salvador, P.; Dannenberg, J. J.; Zakrzewski, V. G.; Dapprich, S.; Daniels, A. D.; Strain, M. C.; Farkas, O.; Malick, D. K.; Rabuck, A. D.; Raghavachari, K.; Foresman, J. B.; Ortiz, J. V.; Cui, Q.; Baboul, A. G.; Clifford, S.; Cioslowski, J.; Stefanov, B. B.; Liu, G.; Liashenko, A.; Piskorz, P.; Komaromi, I.; Martin, R. L.; Fox, D. J.; Keith, T.; Al-Laham, M. A.; Peng, C. Y.; Nanayakkara, A.; Challacombe, M.; Gill, P. M. W.; Johnson, B.; Chen, W.; Wong, M. W.; Gonzalez, C.; and Pople, J. A. *Gaussian 03* (Revision D.01); Gaussian, Inc.: Wallingford, CT, 2004.

(18) Frisch, M. J.; Trucks, G. W.; Schlegel, H. B.; Scuseria, G. E.; Robb, M. A.; Cheeseman, J. R.; Scalmani, G.; Barone, V.; Mennucci, B.; Petersson, G. A.; Nakatsuji, H.; Caricato, M.; Li, X.; Hratchian, H. P.; Izmaylov, A. F.; Bloino, J.; Zheng, G.; Sonnenberg, J. L.; Hada, M.; Ehara, M.; Toyota, K.; Fukuda, R.; Hasegawa, J.; Ishida, M.; Nakajima, T.; Honda, Y.; Kitao, O.; Nakai, H.; Vreven, T.; Montgomery, J. A., Jr.; Peralta, J. E.; Ogliaro, F.; Bearpark, M.; Heyd, J. J.; Brothers, E.; Kudin, K. N.; Staroverov, V. N.; Kobayashi, R.; Normand, J.; Raghavachari, K.; Rendell, A.; Burant, J. C.; Iyengar, S. S.; Tomasi, J.; Cossi, M.; Rega, N.; Millam, J. M.; Klene, M.; Knox, J. E.; Cross, J. B.; Bakken, V.; Adamo, C.; Jaramillo, J.; Gomperts, R.; Stratmann, R. E.; Yazyev, O.; Austin, A. J.; Cammi, R.; Pomelli, C.; Ochterski, J. W.; Martin, R. L.; Morokuma, K.; Zakrzewski, V. G.; Voth, G. A.; Salvador, P.; Dannenberg, J. J.; Dapprich, S.; Daniels, A. D.; Farkas, O.; Foresman, J. B.; Ortiz, J. V.; Cioslowski, J.; Fox, D. J. *Gaussian 09* (Revision D.01); Gaussian Inc.: Wallingford, CT, 2009.

(19) Andrae, D.; Häußermann, U.; Dolg, M.; Stoll, H.; Preuß, H. *Theor. Chim. Acta* **1990**, *77*, 123–141.

(20) (a) Hariharan, P. C.; Pople, J. A. *Theor. Chim. Acta* **1973**, *28*, 213–222. (b) Hehre, W. J.; Ditchfield, R.; Pople, J. A. *J. Chem. Phys.* **1972**, *56*, 2257.

(21) (a) Becke, A. D. *Phys. Rev. A: At., Mol., Opt. Phys.* **1988**, *38*, 3098. (b) Perdew, J. P. *Phys. Rev. B: Condens. Matter Mater. Phys.* **1986**, *33*, 8822–8824.

(22) Tomasi, J.; Mennucci, B.; Cammi, R. *Chem. Rev.* **2005**, *105*, 2999–3094.

(23) Grimme, S.; Antony, J.; Ehrlich, S.; Krieg, H. *J. Chem. Phys.* **2010**, *132*, 154104.